Analysis of Millimeter-Wave Exposure on Rabbit Eye Using a Hybrid PMCHWT-MoM-FDTD Method

Jerdvisanop Chakarothai †, Yukihisa Suzuki †, Masao Taki †, Kanako Wake ‡, Kensuke Sasaki ‡, Soichi Watanabe ‡ and Masami Kojima §

† Tokyo Metropolitan University, 1-1 Minami-Osawa, Hachioji-shi, Tokyo, Japan 192-0397

‡ National Institute of Information and Communication, 4-2-1 Nukui-Kitamachi, Koganei, Tokyo, Japan 184-0015

§ Kanazawa Medical University, 1-1 Daigaku, Uchinada-machi, Ishikawa, Japan 920-0293

Email: † jerd@tmu.ac.jp

***Abstract*-In order to investigate thresholds of biological effects due to millimeter-wave (MMW) exposure, A hybrid method, which combines the Poggio-Miller-Chang-Harrington-Wu-Tsai method of moments (PMCHWT-MoM) and the finite-difference time-domain (FDTD) method, has been developed and applied to analysis of millimeter-wave exposure on rabbit eye using dielectric lens antenna as an electromagnetic source. The PMCHWT MoM has been validated by comparison of calculated and measured electric fields radiated from the dielectric lens antenna. Then, the hybrid PMCHWT-MoM-FDTD method is used to determine specific absorption rate due to MMW exposure on rabbit eye, which was placed at the focal point of the antenna. It was found that the dielectric lens antenna with an input power of 10 mW produces a peak SAR of 86 W/kg in the eye cornea at 35 GHz.**

I. INTRODUCTION

With recent advances in electromagnetic (EM) field technology, the application of millimeter-waves (MMWs) is increasing in daily life, ranging from wireless communications to intelligent transport system such as automobile collision-prevention radar. The rapid development of these new technologies increases public concern about possible biological effects due to EM exposure in millimeter-wave range.

Safety guidelines on EM field exposures published by various organization, including the International Committee on Electromagnetic Safety (ICES) of the Institute of Electrical and Electronics Engineers (IEEE) [1] and the International Commission on Non-Ionizing Radiation Protection (ICNIRP) [2], cover the frequency range of MMWs, i.e., up to 300 GHz. These guidelines are based on established scientific evidence. Few studies, however, address the rationale for the exposure limits in MMW band. The limit values for MMW exposure were derived primarily from extrapolations of experimental data for frequencies up to several GHz, or from the effects of infrared radiation. To confirm the scientific basis for the exposure limit in the MMW region, it is necessary to perform experiments to obtain reliable evidences in this region.

Experimental research in the MMW region, which occupies a broad frequency range from 30 GHz to 300 GHz, however, is difficult from the practical viewpoint due to limit number of animal individuals used in experiments and availability of EM sources in this frequency region. Therefore, the simulation based on actual physical model for calculating power absorption of EM waves into biological bodies is needed.

In this paper, a hybrid method, which combines the Poggio-Miller-Chang-Harrington-Wu-Tsai (PMCHWT) formulation of the method of moments (MoM) [3] and the finite-difference time-domain (FDTD) method [4], is proposed to analyze an exposure system using dielectric lens antenna as an EM source in a MMW range. We are investigating the relationship between injuries for ocular tissues and exposure level of MMW by using rabbit eyes. Since biological effects for MMW exposure is mainly due to EM power absorbed at surface of biological bodies and eyes are considered most vulnerable to MMW [5], [6]. Hence, bare rabbit eye model is employed for our target of numerical simulation. This paper is organized as follows: First, we briefly describe a hybridization of the PMCHWT-MoM and the FDTD method. The PMCHWT MoM is then experimentally validated for a dielectric lens antenna model. Finally, we use the hybrid PMCHWT-MoM-FDTD method to calculate the specific absorption rate (SAR) in rabbit eye by MMW exposure at 35 GHz.

II. HYBRIDIZATION OF PMCHWT-MOM AND FDTD METHOD

The concept of the hybrid PMCHWT-MoM-FDTD method is illustrated in Fig. 1. There are two analysis regions; one is the MoM region including homogeneous dielectrics and metal structures, and the other is the FDTD region including only heterogeneous bodies, e.g. biological bodies. The PMCHWT MoM is applied in the MoM region in order to solve a radiation/scattering problem including dielectric objects. $\mathbf{J}_a$, $\mathbf{J}_d$, and $\mathbf{M}_d$ are electric current density residing on an antenna, electric and magnetic current densities residing on a dielectric structure, respectively. Electric and magnetic current densities on a closed surface S_{JM} surrounding an object in the FDTD region are denoted by $\mathbf{J}_s$ and $\mathbf{M}_s$, respectively. S_{JM} can be chosen arbitrarily as long as it totally encompasses the object. Calculation procedures of the PMCHWT-MoM-FDTD method are as follows:

1) Apply an incident voltage at the antenna terminal, and then $\mathbf{J}_a$, $\mathbf{J}_d$, and $\mathbf{M}_d$ are determined from the MoM procedures. It is assumed that the exposed subject is outside the MoM region and excluded from the calculation.

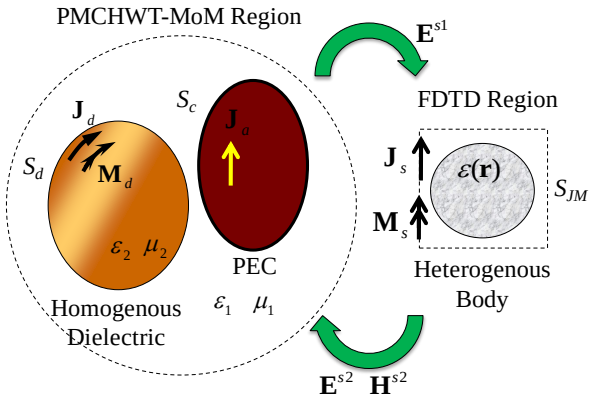

Fig. 1 Concept of a hybrid PMCHWT-MoM-FDTD method.

2) Radiated/scattered electric fields $\mathbf{E}^{s1}$ is calculated for observation points in the FDTD region. Since the solutions of the MoM are found in the frequency domain, we then transform them into the time-domain sinusoidal waveform in order to apply them to the FDTD method as the incident field.

3) Scattered electric and magnetic fields are calculated with the FDTD method. The structures in the MoM region are excluded from the calculation in this step and the perfectly matched layer (PML) is applied at the border of computation space to absorb the outgoing EM fields. The SAR is also calculated from

$$\text{SAR} = \frac{\sigma|\mathbf{E}|^2}{2\rho}, \qquad ...(1)$$

where $\mathbf{E}$ is the peak values of the total electric field (V/m), σ and ρ represent the conductivity (S/m) and the mass density of the tissue (kg•m^{-3}), respectively.

4) $\mathbf{J}_s$ and $\mathbf{M}_s$ on a closed surface surrounding the exposed object are obtained from scattered electric and magnetic fields using the equivalence principle:

$$\mathbf{J}_s = \hat{n} \times \mathbf{H}^s, \mathbf{M}_s = \mathbf{E}^s \times \hat{n}. \qquad ...(2)$$

Since the cell size in the FDTD method is small, actually on the order of one-tenth to -twentieth of wavelength, electric and magnetic dipole moments on a face of the Yee's cell can be considered infinitesimal and can be expressed as

$$\mathbf{j}_p = \mathbf{J}_s(\mathbf{r}_p')\Delta s, \mathbf{m}_p = \mathbf{M}_s(\mathbf{r}_p')\Delta s, \qquad ...(3)$$

where $\mathbf{r}_p'$ is defined as the center coordinate of the small area Δs which corresponds to a face area of the Yee's cell. The scattered electric and magnetic fields at an observation point outside the volume enclosed by S_{JM} can be analytically computed from the following expressions:

$$\mathbf{E}^{s2}(\mathbf{r}) = -jk_0 \sum_{p=1}^{N_d} \frac{e^{-jk_0R_p}}{4\pi R_p}\left\{\eta_0(\mathbf{j}_p - \mathbf{p}_p) + \frac{\eta_0 D}{jk_0}(\mathbf{j}_p - 3\mathbf{p}_p) - D(\mathbf{R}_p \times \mathbf{m}_p)\right\}, \qquad ...(4)$$

$$\mathbf{H}^{s2}(\mathbf{r}) = -jk_0 \sum_{p=1}^{N_d} \frac{e^{-jk_0R_p}}{4\pi R_p}\left\{\frac{1}{\eta_0}(\mathbf{m}_p - \mathbf{p}_p') + \frac{D}{jk_0\eta_0}(\mathbf{m}_p - 3\mathbf{p}_p') + D(\mathbf{R}_p \times \mathbf{j}_p)\right\}, \qquad ...(5)$$

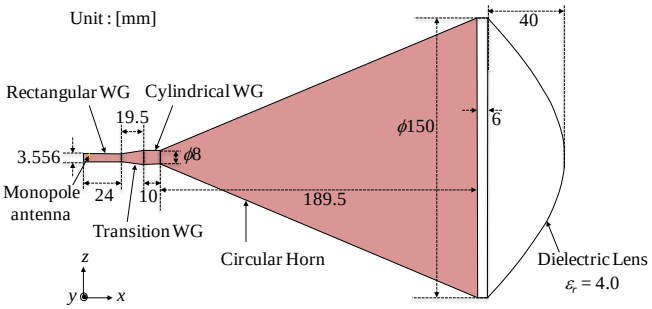

Fig. 2. Structure of the dielectric lens antenna.

$$\mathbf{p}_p = \frac{(\mathbf{R}_p \cdot \mathbf{j}_p)\mathbf{R}_p}{R_p^2}, \mathbf{p}_p' = \frac{(\mathbf{R}_p \cdot \mathbf{m}_p)\mathbf{R}_p}{R_p^2}, D = \frac{1}{R_p}\left(1 - \frac{j}{k_0 R_p}\right),$$

$$\mathbf{R}_p = \mathbf{r} - \mathbf{r}_p,$$

where N_d is a total number of dipole moments.

5) Induced voltages on every edge element in the MoM region are calculated using electric and magnetic fields in (4) and (5) as incident fields. Since they are treated as additional sources in the PMCHWT MoM, $\mathbf{J}_a$, $\mathbf{J}_d$, and $\mathbf{M}_d$ obtained in this step must be added to those obtained in the previous iterations. Steps 2-5 are then repeated until the convergence is reached.

III. Experimental Validation of Dielectric Lens Antenna

A. *Structure of Dielectric Lens Antenna*

Fig. 1 shows the structure of dielectric lens antenna used in numerical analysis. The dielectric lens antenna is composed of rectangular waveguide (WG) with a monopole antenna inside, transition WG, cylindrical WG, circular horn, and dielectric lens. Aperture size of the rectangular WG for Ka band (26.5 GHz to 40 GHz) is 7.112 mm × 3.556 mm. The monopole antenna has a length of quarter wavelength at 35 GHz, i.e., 2.143 mm. An aperture diameter of the cylindrical WG is 8 mm and the tapered part of the horn has a length of 189.5 mm. An aperture diameter of the horn at the open end is 150 mm. Relative permittivity and conductivity of the dielectric lens is 4.0 and 0.001 S/m, respectively. All components are put together in a serial connection as shown in Fig. 1. Analysis frequency is fixed to 35 GHz for all numerical simulations and experiments.

The horn antenna, including the rectangular, transition, and cylindrical waveguides was discretized into 31060 triangular patches while there are 38598 triangular patches for the dielectric lens. Total number of unknowns in the model is 123,659. The PMCHWT MoM code developed in-house was parallelized by adopting the OpenMP interface software platform. The parallelized version of the LU decomposition in the Intel Mathematical Kernel Library (IMKL) was used to accelerate the calculation. All numerical analyses were performed on a high-performance computer with 48 cores (CPU Opteron 6174) in our laboratory. Calculation time for the model was approximately 4 hours and 40 minutes using about 256 GBytes.

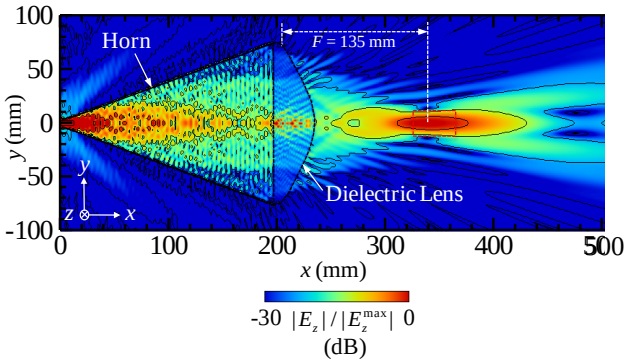

Fig. 3. Near *E*-field distribution in the *xy*-plane at 35 GHz.

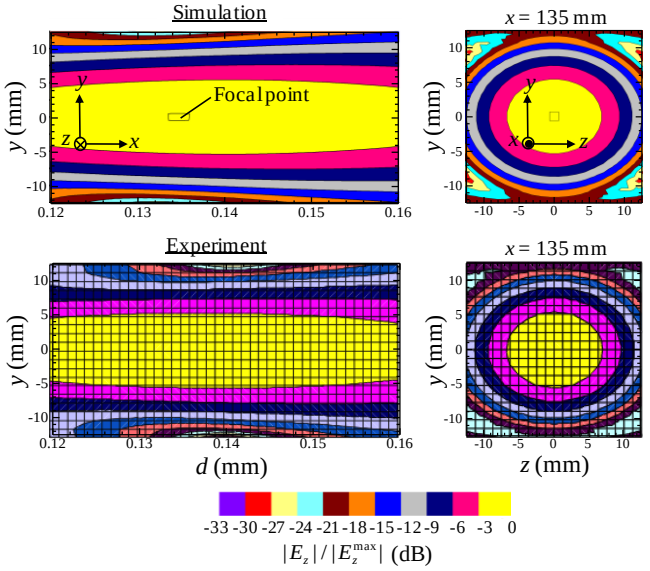

Fig. 4. Comparison of normalized electric field distribution at the focal point of dielectric lens in the *xy*-plane (left) and *yz*-plane (right) at 35 GHz. *d* is the distance from the base of dielectric lens to an observation point.

B. Numerical Analysis and Experimental Validation

First, we calculate electric field distribution created by the dielectric lens antenna. Fig. 3 shows the normalized electric field strength in the *xy*-plane. The focusing behavior of EM waves by dielectric lens can be clearly observed. Focal point of the dielectric lens is then determined as d = 135 mm with a beam width of 10.5 mm × 12.8 mm (half power value), where d is the distance from the base of the dielectric lens. The input impedance of the monopole antenna is 37.12 – j51.06 Ω. The maximum electric field strength, and power density at the focal point are determined as 86.69 V/m and 2.00 mW/cm^2, respectively, for an antenna input power of 4.66 mW. The electric field distribution was also measured by using near-field measurement system (NSI2000, Nearfield System, Inc.). Fig. 4 shows the normalized electric field strength at the focal point in the *xy*-plane and *yz*-plane, calculated by the PMCHWT MoM and measured experimentally, respectively. It can be seen that the numerical results are almost identical to those of the experiment. Fig. 5 shows the electric field strength on the

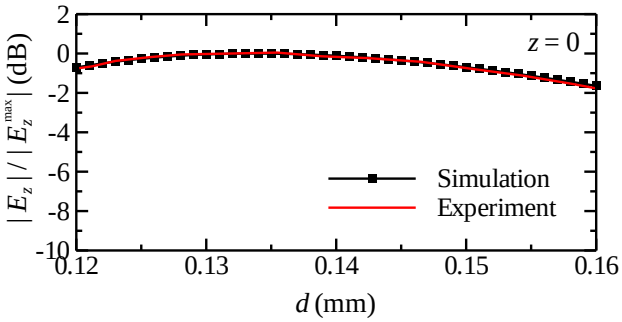

Fig. 5. Comparison of normalized electric field distribution, on the *x*-axis, calculated by the PMCHWT MoM and that obtained from the experiments.

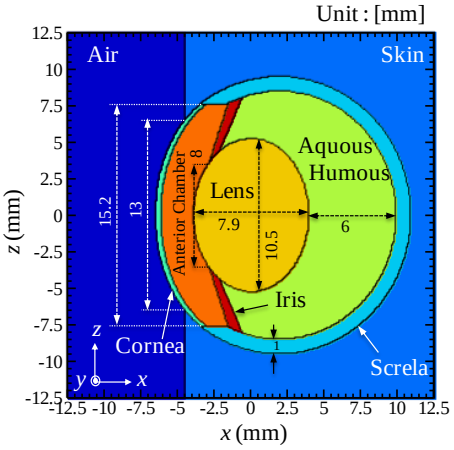

Fig. 6. Structure of eye used in numerical analysis

x-axis when z = 0. Again, the numerical result shows good agreement with the experiment, demonstrating the validity of our PMCHWT MoM.

IV. Numerical Experiment of Millimeter-Wave Exposure on Rabbit Eye

The validity of the PMCHWT MoM has been demonstrated in comparison with the measured electric fields. We then combine the PMCHWT MoM with the FDTD method in order to analyze millimeter-wave exposure on rabbit eye. Since eye has a complex and fine structure as shown in Fig. 6, we have modeled the eye in the FDTD region with a spatial grid size of 0.05 mm in each axis. The eye is placed at the focal point of the dielectric lens. There are 7 types of tissues used in the eye model and their dielectric constants are tabulated in Table I. Dimensions of the FDTD region are 25 mm × 25 mm × 25 mm. The 8-layer perfectly matched layer (PML) is utilized to absorb the outgoing wave in order to truncate the FDTD region. The time step size is 96.29 fs and the number of time steps is 2000. Calculation time for the eye model was approximately 2 hours and 40 minutes using about 62 GBytes.

First, the radiated/scattered electric fields calculated from the PMCHWT MoM, when only the dielectric lens antenna exists in the analysis region, are used as incident fields in the FDTD

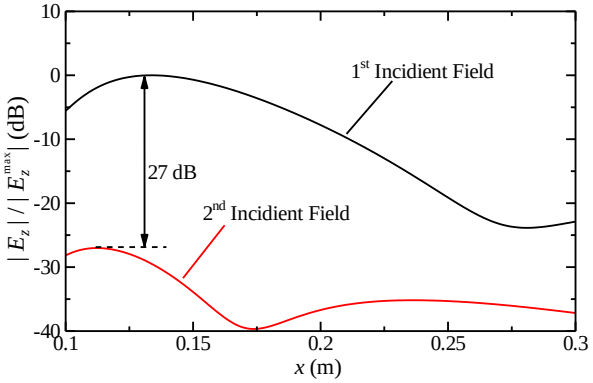

Fig. 7. Distribution of the incident electric fields in the 1st and 2nd iterations of the PMCHWT-MoM-FDTD method.

TABLE I
DIELECTRIC PROPERTIES OF EYE'S TISSUES AT 35 GHZ

	ε_r	σ (S/m)	ρ (kg·m^{-3})
Dry skin	13.34	29.76	1100
Eye sclera	18.87	38.69	1032
Cornea	18.39	37.77	1051
Vitreous humor	22.40	58.53	1005
Lens	16.46	32.34	1076
Anterior chamber	22.41	58.53	1005
Iris	20.42	39.65	1090

region. The SAR is then calculated using the FDTD method. The electric and magnetic fields scattered from the eye, calculated using (4) and (5) are used as a new source for the PMCHWT MoM. We repeated the calculation procedure until the convergence of the SAR is reached. As a result, only two iterations is needed in order to satisfy the convergence condition, since the coupling between the eye and the dielectric lens antenna is quite small. Fig. 7 shows the incident electric field distribution on the *x*-axis in each iteration step. For the 2nd iteration step, the maximum of the electric field strength is approximately 27 dB less than that in the 1st iteration step. Therefore, only one iteration would be sufficient for simulating our numerical exposure experiment

Finally, the SAR distribution calculated by using the hybrid PMCHWT-MoM-FDTD method after two iterations is shown in Fig. 8. The maximum SAR is approximately 40.1 W/kg for an antenna input power of 4.66 mW. As can be seen from the figure, the power absorption of EM wave occurred only nearby the eye surface where it is exposed to the air region. However, the temperature rise due to the MMW exposure would cause a thermal convection inside the anterior chamber of the eye and this may induce the damages inside the eye [7]. This phenomenon will be taken into account in our future research.

V. CONCLUSIONS

In this paper, a hybrid method combining the PMCHWT-MoM and the FDTD method has been proposed to simulate a situation of the MMW exposure on the eye at 35 GHz. The validity of the PMCHWT-MoM has been confirmed by

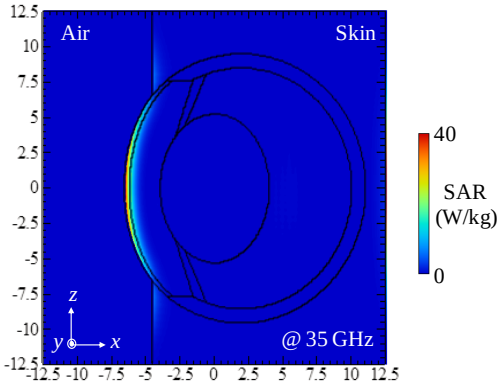

Fig. 8. SAR distribution calculated by using the PMCHWT-MoM-FDTD method. The antenna input impedance is 35.60 – j50.55 Ω and the input power is 4.66 mW.

comparing the calculated electric field distributions with those obtained from the experiment. Then, the PMCHWT-MoM-FDTD method was used in order to determine a power absorbed into the eye and the maximum SAR is determined as 86 W/kg for an antenna input power of 10 mW. It was also confirmed that the coupling between the dielectric lens antenna and the eye is small so that only one iteration will be sufficient for analyses.

A future subject is to include the thermal convection effects into our model and determine thresholds of biological effects in the MMW frequency range.

ACKNOWLEDGMENT

This study was supported in part by Ministry of Internal Affairs and Communications, Japan.

REFERENCES

[1] IEEE International Committee on Electromagnetic Safety, IEEE standard for safety levels with respect to human exposure to radio frequency electromagnetic fields, 3 kHz to 300 GHz, Piscataway, NJ: IEEE; IEEE Std C95.1-2005; 2005.

[2] International Commission on Non-Ionizing Radiation Protection, Guidelines for limiting exposure to time-varying electric, magnetic, and electromagnetic fields (up to 300 GHz), *Health Phys.*, vol. 74, pp. 494-522; 1998.

[3] E. Arvas, A. Rahhal-Arabi, A. Sadigh, and S. M. Rao, "Scattering from multiple conducting and dielectric bodies of arbitrary shape," *IEEE Trans. Antennas Propag. Mag.*, vol. 33, no. 2, pp. 29-36, 1991

[4] A. Taflove, *Computational Electrodynamics: The Finite-Difference Time-Domain Method*, Norwood, MA: Artech House, 1995.

[5] S. W. Rosenthal et. al., *Biological effects of electromagnetic waves vol.1*, Johnson C. C. & Shore M. L., Ed., HEW Publication (FDA) 77-8010, Rockvill, Maryland, 110-128.

[6] H. A. Kues, S. A. D. Anna, R. Osiander, W. R. Green, and J. C. Monahan, "Absence of ocular effects after either single or repeated exposure to 10 W/cm^2 from a 60 GHz CW source," *Bioelectromagnetics*, vol. 20, no. 8, pp. 463-473, 1999.

[7] M. Kojima, M. Hanazawa, Y. Yamashiro, H. Sasaki, S. Watanabe, M. Taki, Y. Suzuki, A. Hirata, Y. Kamimura, and K. Sasaki, "Acute ocular injuries caused by 60 GHz millimeter-wave exposure," *Health Physics*, vol. 97, no. 3, pp. 212-218, 2009.